

Cite this: *Chem. Sci.*, 2023, **14**, 7355

All publication charges for this article have been paid for by the Royal Society of Chemistry

Received 15th May 2023  
Accepted 10th June 2023

DOI: 10.1039/d3sc02461j

rsc.li/chemical-science

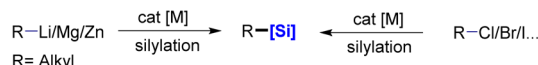
## Introduction

Organosilanes not only play pivotal roles in medicinal chemistry<sup>1</sup> and material science,<sup>2</sup> but they are also highly functionalized and versatile building blocks for further transformation in synthetic chemistry.<sup>3</sup> In the past few decades, considerable attention has been placed on developing synthetic strategies to construct C(sp<sup>3</sup>)-Si bonds by cross-coupling reactions in the presence of transition metals, such as palladium, nickel, and copper salts, as catalysts (Fig. 1A).<sup>4</sup> Highly reactive organometallic species, including Grignard reagents, organolithiums, organozincs or ganoaluminums, are emerging as the most attractive substrates for the construction of organosilanes.<sup>5,6</sup> Although these transformations are synthetically useful, these organometallic reagents exhibit a high basicity and strong nucleophilicity, making them incompatible with many functional groups. Organohalides are often used as precursors to organometallic reagents; therefore, substantial progress has been recently achieved to access silicon-containing molecules by cross-coupling from these abundant and structurally diverse feedstocks to replace preformed organometallic reagents.<sup>7,8</sup> Despite these advances, a method to easily prepare

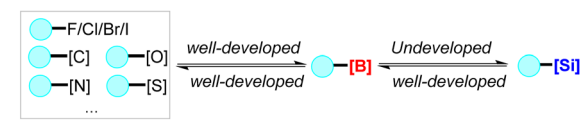
organosilanes without reactive coupling partners and metal catalysts is more attractive.

Interconversion of the main group elements has been a long-standing goal in organic chemistry.<sup>9</sup> In this area, organoboron compounds have become valuable building blocks in organic synthesis because of their flexibility, as they can be synthesized from multiple different functional groups.<sup>10</sup> Significant developments have been achieved for the interconversion of carbon-boron bonds to carbon–carbon and carbon–heteroatom (F, Cl, Br, I, O, N, S ...) bonds (Fig. 1B).<sup>11,12</sup> In this context, the conversion of C-Si bonds into C-B bonds has been developed through the reaction with boron trihalides (BCl<sub>3</sub>, BBr<sub>3</sub>).<sup>13</sup> At the

### (A) Reported routes to organosilanes



### (B) Interconversion of the main group elements



### (C) Opening the route from organoborons to silanes (this work)



<sup>a</sup>School of Chemistry and Molecular Engineering, Nanjing Tech University, Nanjing, 211816, China. E-mail: iasjfh@njtech.edu.cn

<sup>b</sup>State Key Laboratory of Coordination Chemistry, School of Chemistry and Chemical Engineering, Nanjing University, Nanjing, 210023, China

† Electronic supplementary information (ESI) available. See DOI: <https://doi.org/10.1039/d3sc02461j>

Table 1 Effect of reaction parameters<sup>a</sup>

Entry	Variation from standard conditions	Yield <sup>b</sup> (%)
	None	92 (84 <sup>c</sup> )
	Without KO <sup>t</sup> Bu	0
	KOMe instead of KO <sup>t</sup> Bu	21
	NaO <sup>t</sup> Bu instead of KO <sup>t</sup> Bu	Trace
	LiO <sup>t</sup> Bu instead of KO <sup>t</sup> Bu	0
	KOH instead of KO <sup>t</sup> Bu	0
	K <sub>3</sub> PO <sub>4</sub> instead of KO <sup>t</sup> Bu	0
	Toluene as the solvent	69
	<sup>n</sup> Octane as the solvent	58
	MeCN as the solvent	0
	DMF as the solvent	Trace
	At 80 °C	64

<sup>a</sup> Reaction conditions: **1a** (0.4 mmol), **2a** (0.8 mmol), 2 equiv. of KO<sup>t</sup>Bu in THF (2 mL), 5 h, at 100 °C under Ar. <sup>b</sup> The yields were determined by GC-MS analysis using an internal standard. <sup>c</sup> Isolated yield.

Table 2 The scope of alkylborons<sup>abc</sup>

Benzyl substrates <sup>a</sup>	Conditions A or B		Conditions A		Conditions B	
	<b>1</b>	<b>2</b>	<b>3b</b>	<b>3c</b>	<b>3d</b>	<b>3e</b>
<b>3b</b> , 87%						
<b>3c</b> , 65%						
<b>3d</b> , 62%						
<b>3e</b> , 49%						
<b>3f</b> , 57%						
<b>3g</b> , 72%						
<b>3h</b> , 90%						
<b>3i</b> , 61%						
<b>3j</b> , 67%						
<b>3k</b> , 79%						
<b>3l</b> , 83%						
<b>3m</b> , 85%						
<b>3t</b> , 74%						
<b>3u</b> , 77%						
<b>3v</b> , 79% (82%)						
<b>3w</b> , 77%						
<b>3x</b> , 42%						
<b>3y</b> , 45%						
<b>3z</b> , 46%						
<b>3a</b> , 87%						
<b>3b</b> , 80%						
<b>3c</b> , 68%						
<b>3d</b> , 69%						
<b>3e</b> , 55%						
<b>3f</b> , 57%						
<b>3g</b> , 49%						
<b>3h</b> , 52%						
<b>3i</b> , 81%						
<b>3j</b> , 62%						
<b>3k</b> , 65%						
<b>3l</b> , 80%						
<b>3m</b> , 72%						
<b>3n</b> , 89%						
<b>3o</b> , 83%						
<b>3p</b> , 67%						
<b>3q</b> , trace						
<b>Scope of chlorosilanes<sup>b</sup></b>						
<b>3r</b> , 77%						
<b>3s</b> , 70%						
<b>3t</b> , 65%						
<b>3u</b> , 64%						
<b>3v</b> , 64%						
<b>3w</b> , 64%						
<b>3x</b> , 56%						
<b>3y</b> , 43%						
<b>3z</b> , 70%						
<b>3aa</b> , 53%						
<b>3ab</b> , 73%						
<b>3ac</b> , 71%						

<sup>a</sup> Reaction conditions: **1** (0.4 mmol), **2a** (0.8 mmol), 2 equiv. of KO<sup>t</sup>Bu in THF (2 mL), 5 h, at 100 °C under Ar. <sup>b</sup> Reaction conditions: **1** (0.4 mmol), **2b** (0.8 mmol), 2 equiv. of KO<sup>t</sup>Bu in <sup>n</sup>octane (2 mL), 5 h, at 100 °C under Ar; yields given refer to isolated yields of product. <sup>c</sup> The reaction was carried out in THF; yields given refer to isolated yields of product.

outset of this project, no inverse approach from C–B bonds to C–Si bonds had been developed.

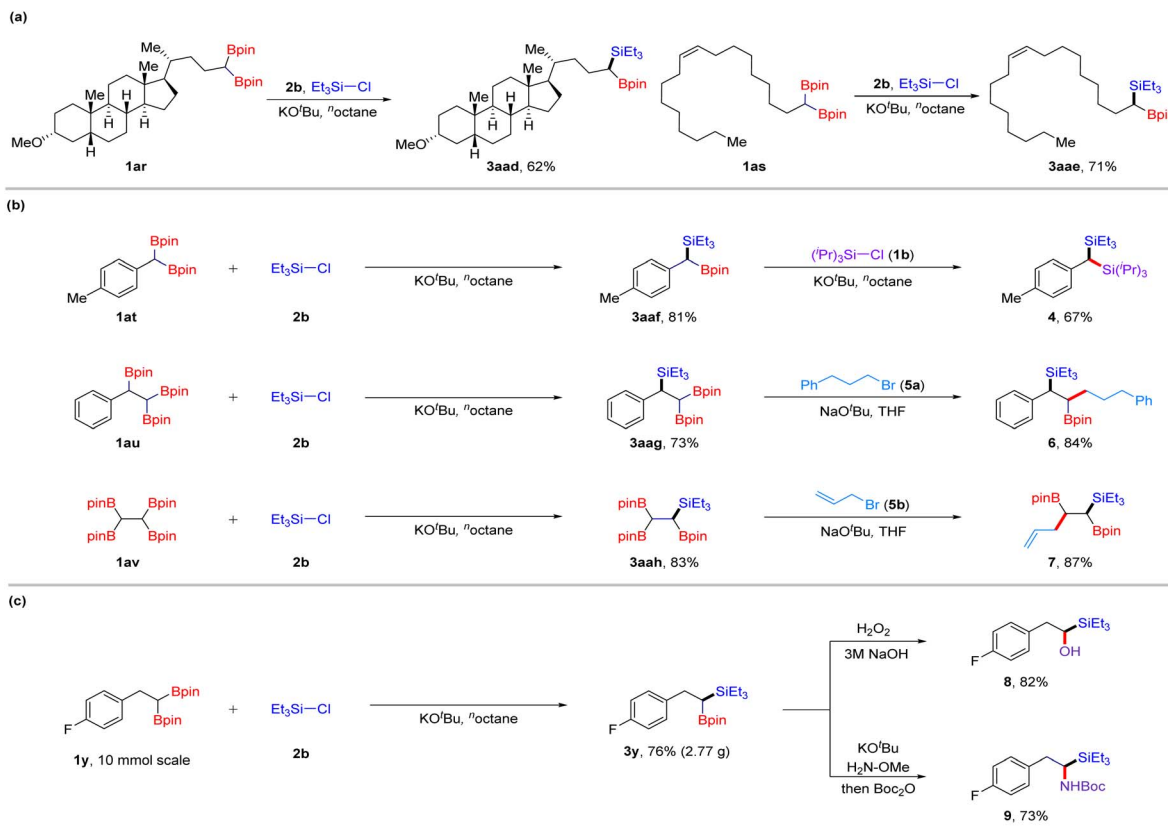
Because of the diagonal relationship between boron and silicon in the periodic table, the boryl and silyl groups exhibit related properties and reactivity for further functionalization, but the latter groups are more stable during storage and

handling.<sup>14</sup> Furthermore, silicon reagents exhibit significant differences in functionality in materials, which are important precursors to commercial polymers and copolymers.<sup>15</sup> Thus, developing a method to prepare organosilanes from related boronates is an attractive goal because it fills the gap in borane–silane interconversion. Here, we develop the first deborylative silylation of benzylic boron esters or multiboronates to organosilanes mediated by an alkoxide base under transition metal-free conditions (Fig. 1C). In this surprisingly simple approach, the *in situ* formation of boron–ate complexes can react with chlorosilanes through a concerted process to access valuable benzyl silanes and silylboronates.

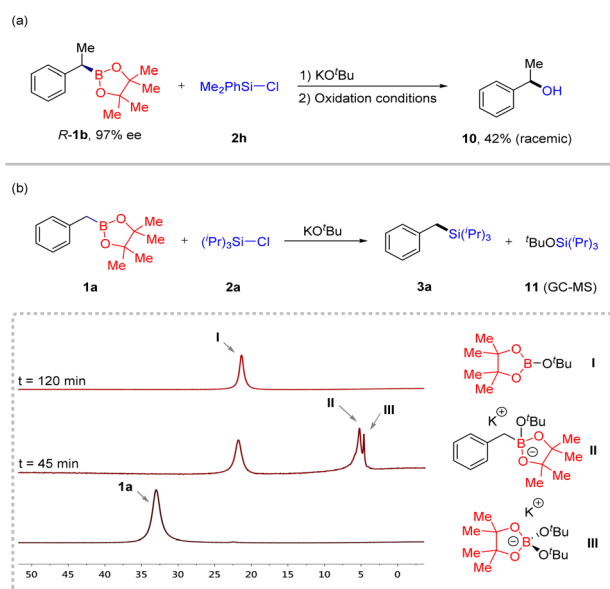
## Results and discussion

We commenced our studies using commercially available 2-benzyl-4,4,5,5-tetramethyl-1,3,2-dioxaborolane **1a** and chlorotriisopropylsilane **2a** as model substrates. Based on a systematic examination of reaction conditions, we determined that the following settings were optimal: KO<sup>t</sup>Bu (2 equiv.) as a base in tetrahydrofuran (THF) at 100 °C. As a result, benzyltriisopropylsilane **3a** was obtained in 84% isolated yield (Table 1, entry 1). KO<sup>t</sup>Bu was removed from standard conditions, and the target product could not be detected by GC-MS (Table 1, entry 2). While **3a** was formed in 21% yield with KOMe (Table 1, entry 3), other commonly used bases, such as NaO<sup>t</sup>Bu, LiO<sup>t</sup>Bu, KOH and K<sub>3</sub>PO<sub>4</sub>, were ineffective for this cross-coupling reaction (Table 1, entries 4–7). These results demonstrated that potassium cations and alkoxide anions are indispensable for the high reactivity of this transformation. When the reaction was conducted in toluene or <sup>n</sup>octane with KO<sup>t</sup>Bu as a base, lower yields were obtained (Table 1, entries 8 and 9). However, other polar solvents, including MeCN and DMF, failed to generate silylated products (Table 1, entries 10–11). Lowering the temperature led to a lower yield with incomplete conversion of the benzyl boron esters, and byproduct *tert*-butoxytriisopropylsilanes (<sup>t</sup>BuO-Si(<sup>i</sup>Pr)<sub>3</sub>) were detected by GC-MS (Table 1, entry 12).

With the optimized conditions in hand, we then evaluated the generality of this method. First, we examined a scope of alkylborons using chlorotriisopropylsilanes or chlorotriethylsilane as coupling partners (Table 2). To our delight, benzyl boronates **1b**–**1m** reacted smoothly with chlorosilanes **2a** under standard conditions, affording benzyl silanes **3b**–**3m** in 49–90% yields. For example, secondary boronates **1b** and **1c** participated in the reactions to obtain corresponding products **3b** and **3c** in 87% and 68% yields, respectively. Naphthalene substrate **1d** was shown to exhibit high levels of reactivity. The products with OMe and OCF<sub>3</sub> groups were formed in acceptable yields (**3e**–**3g**). It should be mentioned that halo substituents, such as F, Cl, Br and I, on the substrates (**1h**–**1k**) did not influence the reaction, indicating their potential application in subsequent cross-coupling transformations. Furthermore, **1l** and **1m** bearing phosphine or ketone substituents on the phenyl group performed well, affording the corresponding products in 83% and 85% yields (**3l** and **3m**, respectively). Remarkably, this strategy could be successfully applied to the



Scheme 1 Synthetic applications of the deboronative silylation.



Scheme 2 Mechanistic experiments.

synthesis of geminal silylboronates,<sup>16</sup> which exhibit unique reactivity characteristics that allow them to participate in a variety of complexity-generating procedures. A range of carbon chain 1,1-bis(pinacolboronate) esters were tolerated under modified conditions, affording valuable silicated boronates in

70–79% yields (3n–3t). In addition, boronates **1u** underwent cross-coupling with chlorotriethylsilane to form highly congested  $\alpha$ -quaternary carbon centres **3u** in 77% yield. Although oxygen-containing substrates participated in this reaction, their yields were low (42–46%; 3v–3x). Substrates possessing fluorine, chlorine, bromine, alkenyl and naphthyl groups were well tolerated in this system (3y–3ad). Delightedly, the common heterocyclic cores could favourably carry out these deboronative cross-coupling transformations (3ae–3ah). Selective functionalization of 1,2-bis(boronate esters) is a challenging topic in organic synthesis.<sup>17</sup> Therefore, we tried the selective cross-coupling reaction with these bis(boronate esters) and chlorosilanes under standard conditions. We found that this cross-coupling exclusively occurs at the benzyl boron, providing 1,2-silylboronates in moderate to good yields (3ai–3ak). Subsequently, 1,1,1-alkyltriboronates and 1,1,2-alkyltriboronates were selectively coupled with chlorosilanes to afford the corresponding products 3al–3ap in 67–89% yield. Most of these silylboronate compounds are difficult to synthesize by known methods. Primary alkylboronates were also examined, but only trace amounts of silanes 3aq were detected by GC-MS.

Next, we investigated the scope of chlorosilanes for cross-coupling with germinal boronates **1aa**. Substrates with different carbon chains were amenable to the cross-coupling reaction as well (3ar–3au). Notably, chlorosilane with a bulky substituent, such as a *tert*-butyl, showed lower yields (3av). The reaction of aryl chlorosilanes could afford target products 3aw,

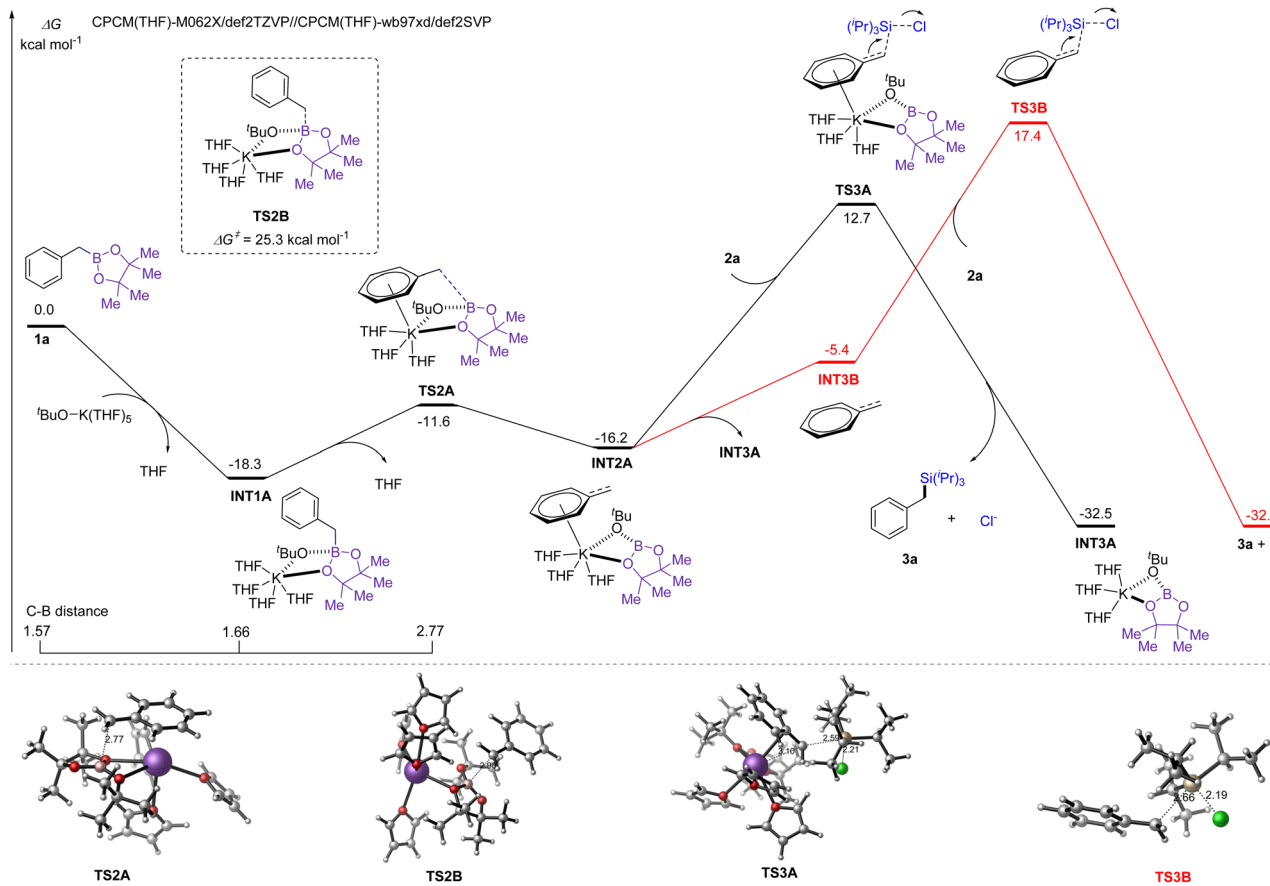


Fig. 2 The calculated energy profiles for the alkoxide-promoted cross-coupling of **1a** and **2a**.

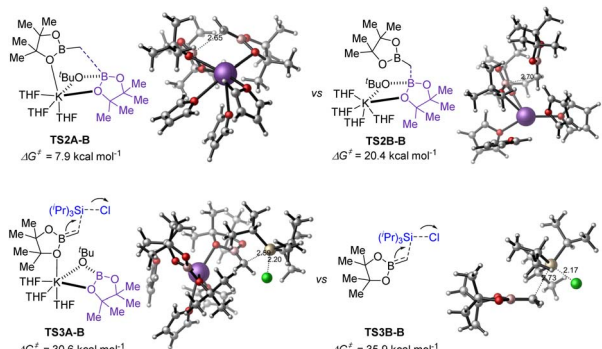


Fig. 3 The additional stabilization for substrate germinal boronates.

**3ax** and **3ay** in satisfactory yields as well. Chlorodisilanes were also feasible substrates with good yields (**3az**). Additionally, the use of a chloro-containing example afforded product **3aaa** in 53% yield. Finally, the presence of alkenyl substituents was tolerated (**3aab** and **3aac**).

To showcase the synthetic applications of this robust deboronative platform, we performed late-stage modification of complex molecules and a series of sequential transformations (Scheme 1). Lithocholic acid derivative **1ar** reacted with  $\text{Et}_3\text{SiCl}$  (**2b**) under optimized conditions, affording product **3aad** in 62% yield. Oleic acid derivative **1as** bearing a *trans*-alkene group

provided silylboronate **3aae** in 71% yield. Interestingly, by continuously treating **1at** with chlorosilanes and  $\text{KO}^\ddagger\text{Bu}$ , two deborylative silylations occurred, affording geminal disilanes **4** in 67% yield. When using 1,1,2-alkyltriborionate **1au** with two reactive sites as a substrate, the selective process of silylation was observed to give triethyl(1-phenyl-2,2-bis(4,4,5,5-tetramethyl-1,3,2-dioxaborolan-2-yl)ethyl) silane **3aag**, which can further undergo cross-coupling with alkyl bromide **5a** under the condition of sodium alkoxide ( $\text{NaO}^\ddagger\text{Bu}$ ),<sup>18</sup> providing 1,2-silylboronate **6** in 84% yield. Moreover, successive silylation and allylation led to the desired (1,2-bis(4,4,5,5-tetramethyl-1,3,2-dioxaborolan-2-yl)pent-4-en-1-yl)triethylsilane **7** in 87% yield. These results demonstrate the excellent chemoselectivity of this method. A gram-scale reaction proceeded with **1y**, affording a 76% isolated yield of silylated product **3y**, which can then undergo oxidation or amination processes to afford hydroxyl- or amino-products (**8**, **9**) in good yields, respectively.

To determine the reaction mechanism, we performed some experiments (Scheme 2). First, when **R-1b** (97% ee) was reacted with  $\text{Me}_2\text{PhSi-Cl}$  (**2h**) under our conditions, racemic compound **10** was observed in 42% yield after oxidation treatment. GC-MS was used to detect the course of the reaction, and we found that byproduct **11** formed. Subsequently, *in situ*  $^{11}\text{B}$  NMR of the reaction process was performed using benzyl boron ester **1a** and chlorosilane **2a** as substrates, and three new resonances (**I**, **II**, and **III**) appeared at 45 minutes. The resonance at 5.1 ppm (**II**) is

assigned to an “ate” complex.<sup>19</sup> Over time, this characteristic peak gradually disappeared. Based on these observations, we speculate that this transformation involves two processes. The first step was the generation of a carbanion through a deborylative pathway of an “ate” complex **II**. The second step was the nucleophilic reaction of the formed alkyl anion with chlorosilane to generate the final product.

The proposed mechanism was further supported by a detailed density functional theory (DFT) study, as shown in Fig. 2. Initially, the boron atom of **1a** is coordinated with the oxygen of  $\text{KO}^\ddagger\text{Bu}$  solvated by five tetrahydrofuran molecules, and then the oxygen of **1a** replaces one molecule of THF at potassium to generate **INT1A** with an exothermic energy of  $18.3 \text{ kcal mol}^{-1}$ . In **INT1A**, the boron centre is more electron-rich than that in **1a**, and the C–B distance is elongated to  $1.66 \text{ \AA}$  from  $1.57 \text{ \AA}$ , decreasing the bond dissociation energy of the C–B bond. Subsequent C–B bond cleavage proceeds smoothly through transition state **TS2A** with an energy barrier of  $6.7 \text{ kcal mol}^{-1}$ , in which the potassium cation binds to the aromatic ring of **1a** to stabilize the developing negative charge centre and simultaneously release one molecule of THF. The direct cleavage of the C–B bond *via* transition state **TS2B** without the assistance of potassium requires a higher activation free energy ( $25.3 \text{ kcal mol}^{-1}$ ). The negative charge centre in intermediate **INT2A** undergoes nucleophilic attack to chlorotriisopropylsilane **2a** *via* transition state **TS3A** with an activation free energy of  $28.9 \text{ kcal mol}^{-1}$ , producing the desired alkyl silane **3a** and byproduct **INT3A**. The calculational results indicate that the nucleophilic attack step is the rate-determining step, and the overall activation free energy for this transformation is  $31.0 \text{ kcal mol}^{-1}$ . The nucleophilic attack step for the alkyl anion released from **INT2A** must overcome an overall free energy of  $35.7 \text{ kcal mol}^{-1}$  through transition state **TS3B**, which is  $4.7 \text{ kcal mol}^{-1}$  higher than that of **TS3A**. This explains why the deborylative silylation can be promoted by  $\text{KOMe}$  but failed with sodium alkoxide or lithium alkoxide (Table 1, entries 3–5). Therefore, both the alkoxide anion and potassium cation are indispensable in this transformation, as these entities participate in the formation of a more stable intermediate species, lowering the energy barrier of C–B bond cleavage and C–Si bond formation.

For substrate germinal boronates, the pathways for C–B bond cleavage through transition **TS2A–B** and the subsequent C–Si bond formation *via* **TS3A–B** have the lower energies (Fig. 3). Comparing the energy barrier of transition state **TS3A–B** in the rate-determining step, the stepwise  $\text{S}_{\text{N}}2$  pathway through **TS3B–B** was found to be disfavoured kinetically and ruled out. Overall, DFT analysis further reveals that the transition states **TS2A–B** and **TS3A–B** are substantially stabilized by the coordination between the potassium cation and oxygen of the reserved boronate (see ESI† for details).

## Conclusions

In summary, we have established a general and practical method for synthesizing alkyl silane derivatives from readily available benzylic boronates, geminal bis(boronates) or

alkyltriboronates. This transition-metal-free transformation features excellent chemoselectivity, broad substrate scope, versatility, and scalability. These borylated silanes can readily be further functionalized by well-established organoboron chemistry to enhance the molecular complexity. In view of these features, this transformation should have high synthetic value in the field of materials and pharmaceuticals.

## Data availability

The synthetic procedures, characterization, and spectral data supporting this article have been uploaded as part of the ESI.†

## Author contributions

J. H. conceived the project and directed the research. S. J. and Z. S. supervised the mechanistic study. J. H. and Z. S. wrote the paper. M. T., W. Z., J. W. and H. S. performed the experiments. M. W. performed the DFT calculations.

## Conflicts of interest

The authors declare no competing financial interest.

## Acknowledgements

We are grateful for the financial support from the National Natural Science Foundation of China (21901114), the Start-up Grant from Nanjing Tech University (38274017102) and Tang Scholar. We are grateful to the High Performance Computing Center of Nanjing University for doing the numerical calculations in this paper on its blade cluster system.

## Notes and references

- (a) A. K. Franz and S. O. Wilson, *J. Med. Chem.*, 2013, **56**, 388–405; (b) R. Ramesh and D. S. Reddy, *J. Med. Chem.*, 2018, **61**, 3779–3798.
- (a) R. Pietschnig and S. Spirk, *Coord. Chem. Rev.*, 2016, **323**, 87–106; (b) E. A. Marro and R. S. Klausen, *Chem. Mater.*, 2019, **31**, 2202–2211.
- (a) F. Zhao, S. Zhang and Z. Xi, *Chem. Commun.*, 2011, **47**, 4348–4357; (b) S. E. Denmark and A. Ambrosi, *Org. Process Res. Dev.*, 2015, **19**, 982–994; (c) T. Komiya, Y. Minami and T. Hiyama, *ACS Catal.*, 2017, **7**, 631–651.
- S. Bähr, W. Xue and M. Oestreich, *ACS Catal.*, 2019, **9**, 16–24.
- (a) M. Lacout-Loustalet, J. Dupin, F. Metras and J. Valade, *J. Organomet. Chem.*, 1971, **31**, 187–204; (b) P. J. Lennon, D. P. Mack and Q. E. Thompson, *Organometallics*, 1989, **8**, 1121–1122; (c) A. P. Cinderella, B. Vulovic and D. A. Watson, *J. Am. Chem. Soc.*, 2017, **139**, 7741–7744; (d) B. Vulovic, A. P. Cinderella and D. A. Watson, *ACS Catal.*, 2017, **7**, 8113–8117; (e) S. Mallick, E.-U. Würthwein and A. Studer, *Org. Lett.*, 2020, **22**, 6568–6572.
- (a) K. Tamao, A. Kawachi and K. Ito, *J. Am. Chem. Soc.*, 1992, **114**, 3989–3990; (b) K. Tamao and A. Kawachi, *Adv. Organomet. Chem.*, 1995, **38**, 1–58; (c) C. K. Chu, Y. Liang



and G. C. Fu, *J. Am. Chem. Soc.*, 2016, **138**, 6404–6407; (d) W. Xue, R. Shishido and M. Oestreich, *Angew. Chem., Int. Ed.*, 2018, **57**, 12141–12145; (e) R. Chandrasekaran, F. T. Pulikkottil and K. S. Elama, *Chem. Sci.*, 2021, **12**, 15719–15726.

7 (a) W. Xue, Z.-W. Qu, S. Grimme and M. Oestreich, *J. Am. Chem. Soc.*, 2016, **138**, 14222–14225; (b) W. Xue and M. Oestreich, *Angew. Chem., Int. Ed.*, 2017, **56**, 11649–11652; (c) Y. Takeda, K. Shibuta, S. Aoki, N. Tohnai and S. Minakata, *Chem. Sci.*, 2019, **10**, 8642–8647; (d) J. Scharfbier, B. M. Gross and M. Oestreich, *Angew. Chem., Int. Ed.*, 2020, **59**, 1577–1580.

8 (a) J. Duan, K. Wang, G.-L. Xu, S. Kang, L. Qi, X.-Y. Liu and X.-Z. Shu, *Angew. Chem., Int. Ed.*, 2020, **59**, 23083–23088; (b) L. Zhang and M. Oestreich, *Angew. Chem., Int. Ed.*, 2021, **60**, 18587–18590.

9 (a) D. A. Petrone, J. Ye and M. Lautens, *Chem. Rev.*, 2016, **116**, 8003–8104; (b) K. Ouyang, W. Hao, W.-X. Zhang and Z. Xi, *Chem. Rev.*, 2015, **115**, 12045–12090; (c) L.-J. Cheng and N. P. Mankad, *Chem. Soc. Rev.*, 2020, **49**, 8036–8064; (d) R. Sharma and M. R. Yadav, *Org. Biomol. Chem.*, 2021, **19**, 5476–5500; (e) F. Mo, D. Qiu, L. Zhang and J. Wang, *Chem. Rev.*, 2021, **121**, 5741–5829; (f) A. Varenikov, E. Shapiro and M. Gandelman, *Chem. Rev.*, 2021, **121**, 412–484; (g) S. Huang, M. Wang and X. Jiang, *Chem. Soc. Rev.*, 2022, **51**, 8351–8377.

10 (a) A. J. L. Lennox and G. C. Lloyd-Jones, *Chem. Soc. Rev.*, 2014, **43**, 412–443; (b) A. Fawcett, J. Pradeilles, Y. Wang, T. Mutsga, E. L. Myers and V. K. Aggarwal, *Science*, 2017, **357**, 283–286; (c) J. Hu, Y. Zhao and Z. Shi, *Nat. Catal.*, 2018, **1**, 860–869; (d) X. Liu, W. Ming, Y. Zhang, A. Friedrich and T. B. Marder, *Angew. Chem., Int. Ed.*, 2019, **58**, 18923–18927; (e) J. Li, H. Wang, Z. Qiu, C. Y. Huang and C.-J. Li, *J. Am. Chem. Soc.*, 2020, **142**, 13011–13020.

11 From boron to other main group elements: (a) C. M. Crudden, B. W. Glasspoole and C. J. Lata, *Chem. Commun.*, 2009, 6704–6716; (b) D. Leonori and V. K. Aggarwal, *Angew. Chem., Int. Ed.*, 2015, **54**, 1082–1096; (c) T. C. Wilson, T. Cailly and V. Gouverneur, *Chem. Soc. Rev.*, 2018, **47**, 6990–7005.

12 From other main group elements to boron: (a) E. C. Neeve, S. J. Geier, I. A. I. Mkhald, S. A. Westcott and T. B. Marder, *Chem. Rev.*, 2016, **116**, 9091–9161; (b) M. Wang and Z. Shi, *Chem. Rev.*, 2020, **120**, 7348–7398; (c) J. Hu, M. Ferger, Z. Shi and T. B. Marder, *Chem. Soc. Rev.*, 2021, **50**, 13129–13188.

13 (a) W. Haubold, J. Herdtle, W. Gollinger and W. Einholz, *J. Organomet. Chem.*, 1986, **315**, 1–8; (b) A. A. Kolomeitsev, A. A. Kadyrov, J. Szczepekowska-Sztolcman, M. Milewska, H. Koroniak, G. Bissky, J. A. Bartene and G. Röschenthaler, *Tetrahedron Lett.*, 2003, **44**, 8273–8277; (c) D. L. Crossley, J. Cid, L. D. Curless, M. L. Turner and M. J. Ingleson, *Organometallics*, 2015, **34**, 5767–5774; (d) A. Lik, L. Fritze, L. Müller and H. Helten, *J. Am. Chem. Soc.*, 2017, **139**, 5692–5695; (e) C. You, M. Sakai, C. G. Daniliuc, K. Bergander, S. Yamaguchi and A. Studer, *Angew. Chem., Int. Ed.*, 2021, **60**, 21697–21701; (f) J. Yao, L. Yu, W. Duan and C.-J. Li, *Org. Chem. Front.*, 2023, **10**, 524–530.

14 C. Cheng and J. F. Hartwig, *Chem. Rev.*, 2015, **115**, 8946–8975.

15 A. M. Muzafarov, *Silicon Polymers*, Springer, Heidelberg, 2011.

16 (a) A. A. Szymaniak, C. Zhang, J. R. Coombs and J. P. Morken, *ACS Catal.*, 2018, **8**, 2897–2901; (b) Z. Cheng, J. Guo, Y. Sun, Y. Zheng, Z. Zhou and Z. Lu, *Angew. Chem., Int. Ed.*, 2021, **60**, 22454–22460; (c) Y. You and S. Ge, *Angew. Chem., Int. Ed.*, 2021, **60**, 20684–20688; (d) S. Jin, K. Liu, S. Wang and Q. Song, *J. Am. Chem. Soc.*, 2021, **143**, 13124–13134; (e) W. Sun, L. Xu, Y. Qin and C. Liu, *Nat. Synth.*, 2023, **2**, 413–422.

17 (a) S. N. Mlynarski, C. H. Schuster and J. P. Morken, *Nature*, 2014, **505**, 386–390; (b) R. D. Dewhurst and T. B. Marder, *Nat. Chem.*, 2014, **6**, 279–280; (c) L. Xu, S. Zhang and P. Li, *Chem. Soc. Rev.*, 2015, **44**, 8848–8858.

18 K. Hong, X. Liu and J. P. Morken, *J. Am. Chem. Soc.*, 2014, **136**, 10581–10584.

19 B. Lee and P. J. Chirik, *J. Am. Chem. Soc.*, 2020, **142**, 2429–2437.

